Biogeography Based Optimal State Feedback Controller for Frequency Regulation of a Smart Microgrid

S. Mishra, *Senior Member, IEEE*, G. Mallesham, *Member, IEEE*, and P. C. Sekhar, *Student Member, IEEE*

***Abstract*—Development of "Q" and "R" matrices for designing a Linear Quadratic Regulator (LQR) is still a research challenge. The theory says they should belong to the group of positive definite matrices, so we need to find out the most suitable amongst them in order to obtain the desired response. In this paper biogeography based optimization (BBO) technique has been applied to come up with the best "Q" and "R" matrices such that the frequency excursion following a disturbance in a microgrid is minimized. As all the states in a practical system may not be measurable hence, we have used Kalman estimator to estimate them. These estimated states along with other measured states are used by the LQR to produce the desired control signal. The microgrid is made smarter by using the agent based scheme integrated with a master controller and a proper communication protocol. The simulation results show that the proposed approach improves the microgrid frequency response and also gives a new alternative method for frequency control of a smart microgrid.**

***Index Terms*—BBO, Bryson's method, frequency control, Kalman estimator, LQR, microgrid central controller (MGCC), multi-agent system (MAS), tuning of LQR parameters.**

I. Introduction

INTEGRATION of small capacity power generating sources into the present passive distribution system converts it to an active distribution network [1] and they generally operate in a grid connected mode. However, fault, voltage sags and large frequency oscillations in the main grid, may force them to get disconnected from the main grid and operate as an isolated microgrid [1].

In this situation there will be changes in the power output from the controllable micro sources which need to be regulated properly so that there can be a balance between demand and supply within the isolated microgrid [2]–[4]. The diesel generator, combine cycle gas turbine based system, fuel cell, aqua electrolyzer, battery, wind, etc., can be considered as controllable sources, if available in the microgrid. It is well-known that when there is a mismatch in demand and supply in a power system, the gap is met by inertial energy and hence, the frequency of the system changes. Therefore, in this paper, the power output of the controllable sources is regulated based on the frequency deviation of the microgrid so that in steady state again there will be a match between the demand and supply. This regulation will not be linear due to the inherent time delay and ramp rate limit/generation rate constraint (GRC) associated with the sources. Besides, for proper load sharing among the sources we introduce a power-frequency (P-f) droop (R) for the power generating sources participating in the frequency control [5], [6].

In our previous work [7], the modeling of microgrid and its frequency regulation using proportional and integral (PI) controllers has already been presented. However, many a times the PI controller gives sub-optimal performance as it does not utilize the information about all the internal states of the system.

To overcome this limitation, the LQR has been implemented in many engineering problems [8], [9]. The most challenging issue in designing the LQR lies in finding the weightage matrices "Q" and "R" required by the Riccati equation [10]. Generally, these are decided by some heuristics as proposed by Bryson [11], Johnson and Grimble [12] or by trail and error. However, these conventional methods require many trial and error iterations and may lead to suboptimal solutions. Therefore, to obtain a near global soulution an evolutionary algorithm known as BBO is used to find out the elements of "Q" and "R" matrices. The "Q" and "R" so obtained are used in the Riccati equation to obtain the optimal feedback gain "K." In [13] the concept of BBO has been deliberated where as some interesting engineering applications of it has been presented in [14], [15]. BBO has some similarity with other population based algorithms such as genetic algorithms (GA) [16] and particle swarm optimization (PSO) [17]–[19] with some extra advantages in optimization like, carrying of information from first iteration to next, no reproduction process, the change of solutions directly via migration from other solutions and various others.

In practice it may not be possible to measure all the states required for the solution of the Riccati equation hence, in this paper we have used Kalman estimator to estimate those states for which we do not have any information.

Therefore, the contributions of this paper are as follows.

i. BBO has been used to tune "Q" and "R" matrices for proper regulation of the controllable sources to maintain the frequency in a microgrid. The frequency response of the microgrid with LQR controller tuned with BBO is compared with conventional *(fminsearch)*, GA and PSO.
ii. Providing an efficient energy management strategy as well as keeping proper control and coordination among

Manuscript received August 31, 2011; revised January 23, 2012; accepted December 11, 2012. Paper no. TSG-00433-2011.

The authors are with the Department of Electrical Engineering, Indian Institute of Technology Delhi, New Delhi 110016, India (e-mail: sukumar@ee.iitd.ac.in; malleshamg@yahoo.com; psekhar.chandra@gmail.com).

Color versions of one or more of the figures in this paper are available online at http://ieeexplore.ieee.org.

Digital Object Identifier 10.1109/TSG.2012.2236894

the controllers using the concept of multi agent systems (MAS) (treating each load and source as an agent). Each agent communicates with the other following User Datagram Protocol (UDP/IP) over the internet/intranet.

This paper is organized as follows, Section II illustrates the microgrid modeling and its main components along with the design of P-f droop. Section III presents the state feedback control, output state feedback control and its implementation procedure in the microgrid. In Section IV, a comparative analysis of tuning of "Q" and "R" matrices based on conventional and some evolutionary algorithms has been presented. Section V deliberates on different aspects of BBO. Section VI presents the concept of smart microgrid and its implementation. In Section VII, simulation results are given for various cases. The conclusions are presented in Section VIII.

II. Modeling of Microgrid

The power from the renewable energy based sources fluctuates. Many a times, the generated power is more than the load, in order to store this precious energy we have considered the aqua electrolyzer in the microgrid. The hydrogen produced from the aqua electrolyzer can be stored in a storage tank so that it can be used by the fuel cell to produce electricity whenever the situation demands. On the other extreme, when the generation from the renewable sources become zero the total power required by the load needs to be catered by the controllable sources, otherwise load shedding needs to be carried out. A battery can be considered to improve the damping of frequency excursion following each disturbance by regulating its power during transient period.

So if we assume a 100% self sufficient isolated microgrid, the total rating of the controllable sources should be same as that of the load. Therefore, in this paper we have considered a microgrid, as shown in Fig. 1, consisting of wind power source (305 kW), solar power source (310 kW), load (615 kW), diesel generator (400 kW), fuel cell (200 kW), aqua electrolyzer (100 kW) and battery (30 kWh). As shown in Fig. 1, the communication links between different agents are established based on the internet/intranet. These help in the monitoring and efficient utilization of energy resources in the microgrid as explained in Section VI.

A. The Renewable Energy Sources

1) Wind Energy Conversion System (WECS): In general, for the units participating in the regulation service, irrespective of continuous frequency regulation or contingency, certain amount of generation margin should be kept aside as reserve to facilitate governor actions. This idea has been extended to the wind turbines, which are selected to provide frequency regulation for which the de-loaded operation is necessary [20], [21].

As shown in the Fig. 2, the generated mechanical torque (T_m) is a complex function of wind speed (w_s), rotor speed (w_r), and pitch angle (β). The power coefficient (C_p) value of a wind turbine can be expressed as a fourth order polynomial on λ (tip speed ratio) and β as presented in (1).

$$C_p(\lambda,\beta)=\sum_{i=0}^{4}\sum_{j=0}^{4}\alpha_{i,j}\beta^i\lambda^j. \tag{1}$$

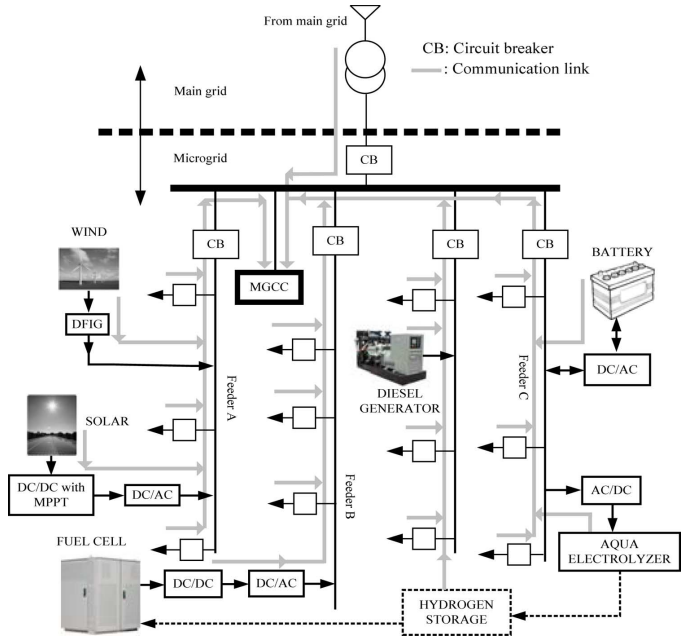

Fig. 1. The basic block diagram of smart microgrid with wind, solar, fuel cell, diesel generator, aqua electrolyzer, and battery.

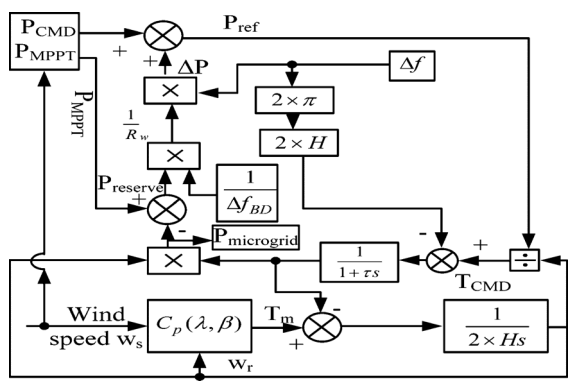

Fig. 2. Block diagram of a WECS model.

The values of the coefficients $\alpha_{i,j}$ are given in [21]. The expression for λ is defined as

$$\lambda=\frac{w_0R_rw_r}{w_s}. \tag{2}$$

where w_r is rotor speed in pu, w_s is wind speed in m/s, w_0 is rotor base speed in rad/s and R_r is rotor radius in meters.

In case of a wind turbine when the output power exceeds the rating of the machine, the pitch angle control is initiated. In this case, it is assumed that the wind speed is such that the power output is always less than its rating and hence, the pitch angle control is absent. As shown in Fig. 2 the $\mathrm{P_{CMD}}$ command, which is 90% of the maximum power available at the wind speed (10% de-rating), is added with an auxiliary signal derived using the frequency deviation and the variable P-f droop $\mathrm{R_w}$ to obtain the reference power $\mathrm{P_{ref}}$. This power reference is further reduced to a torque reference with the help of rotor speed and when added with the inertial response presents the toque command $\mathrm{T_{CMD}}$ to the rotor side converter of the DFIG, injecting the desired power to the microgrid.

2) Solar Panel Modeling Under Maximum Power Point Tracking (MPPT) Operation: The power output from the solar photo voltaic (PV) panel [22] is given by (3)

$$P_{pv} = n_p C S V_{dc} - n_p I_{rs} V_{dc} \left(e^{\alpha V_{dc}} - 1\right). \tag{3}$$

where n_p = number of PV strings in parallel, C = DC-link capacitance, S = solar insolation, V_{dc} = DC-link (PV array) voltage and I_{rs} = reverse saturation current.

The change in PV panel power with respect to a small perturbation in V_{dc} can be written as below,

$$\frac{dP_{pv}}{dV_{dc}} = n_p C S - n_p I_{rs} \left(e^{\alpha V_{dc}} + \alpha V_{dc} e^{\alpha V_{dc}} - 1\right). \tag{4}$$

Equating $dP_{pv}/dV_{dc} = 0$, we can obtain (5) from which the required dc voltage (V_{dc0}) to extract maximum power from the PV panel at any given insolation "S_0" can be calculated.

$$\frac{CS}{I_{rs}} = \left(e^{\alpha V_{dc}} + \alpha V_{dc} e^{\alpha V_{dc}} - 1\right). \tag{5}$$

Now, perturbing (5) around V_{dc0} and S_0 we can reach (6).

$$\Rightarrow \Delta V_{dc} = \frac{C \Delta S}{\left(2\alpha e^{\alpha V_{dc0}} + \alpha^2 V_{dc0} e^{\alpha V_{dc0}}\right) I_{rs}}. \tag{6}$$

Similarly, perturbing (3) around V_{dc0} and S_0 results to (7).

$$\therefore \Delta P_{pv} = \Bigg(n_p C \Delta S V_{dc0} + n_p C \Delta V_{dc} S_0 - n_p I_{rs} \Delta V_{dc} e^{\alpha V_{dc0}} - n_p I_{rs} V_{dc0} \alpha e^{\alpha V_{dc0}} \Delta V_{dc} + n_p I_{rs} \Delta V_{dc} \Bigg). \tag{7}$$

By substituting ΔV_{dc} from (6) in (7), we get

$$\Rightarrow \frac{\Delta P_{pv}}{\Delta S} = K_s = n_p C V_{dc0} + \Big(C S_0 - I_{rs} e^{\alpha V_{dc0}} - I_{rs} V_{dc0} \alpha e^{\alpha V_{dc0}} + I_{rs} \Big) \times \frac{n_p C}{\left[\left(2\alpha e^{\alpha V_{dc0}} + \alpha^2 V_{dc0} e^{\alpha V_{dc0}}\right) I_{rs}\right]}. \tag{8}$$

Now, the challenge is how to find the operating point at which we should perturb so that the gain K_s will be valid for a wide range of insolation. To overcome this challenge we have carried out the following experimentation.

Calculate K_s at 20% insolation. Keeping the K_s unchanged vary S (say $S = 0.3$ and hence $\Delta S = 0.3 - 0.2$) and get ΔP_{pv}, add this ΔP_{pv} to the MPPT power obtained at 20% insolation level. Let this power be termed as estimated power (P_{est}) at $S = 0.3$. Now, calculate the actual power (P_{act}) at this $S = 0.3$ by first obtaining the MPPT V_{dc} from (5) and then substituting that into (3). Now the % error at $S = 0.3$ can be defined as

$$err_s = \frac{100\left(P_{est} - P_{act}\right)}{P_{act}}. \tag{9}$$

Similar exercise can be carried out for the other insolation(s) (such that it covers whole range from 10% to 90%) and % errors are calculated based on (9). The histogram corresponding to % error and insolation level is presented in Fig. 3(a).

Looking at Fig. 3(a), the maximum % error introduced due to the assumption of constant K_s is recorded. Now, the whole procedure is repeated for another insolation, say $S = 0.1$ and maximum % error is obtained. The histogram of maximum % error against solar insolation in the range of 0.1 to 0.9 insolation level is depicted in Fig. 3(b).

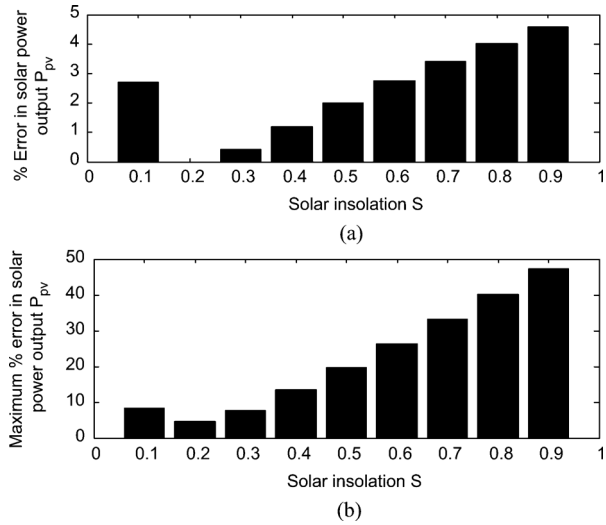

Fig. 3. (a) The percentage error in estimating maximum P_{pv} when K_s is calculated at $S = 0.2$. (b) The maximum percentage error in estimating maximum P_{pv} when K_S is calculated for different solar insolation ranging from 0.1 to 0.9.

Looking carefully at Fig. 3(b), we can conclude that if K_s is calculated at $S = 0.2$, the maximum % error in estimating the P_{pv} is just around 5% in the whole range of operation. Therefore, in this paper we have taken the K_s value corresponding to $S = 0.2$ for all our simulation purposes.

Since, the PV panel is interfaced to the microgrid via a voltage source converter (VSC), its input power can be transferred to its output by the pulse width modulation (PWM) controller in 2–3 cycles. Therefore, the transfer function of a PV panel under MPPT can be represented as in (10).

$$\Delta P_s = \frac{K_s \Delta S}{(1 + sT_s)}. \tag{10}$$

where "T_s" is the time constant of the converter controller and P_s is the electrical power output from the solar system.

B. The Secondary Energy Sources or Controllable Sources Transfer Functions

In this paper, the transfer functions of governor, turbine of the diesel generator, fuel cell, aqua electrolyzer and battery are taken from [23] and are depicted below.

$$\left.\begin{aligned} &G_{dgg}(s) = \tfrac{K_{dgg}}{(1+sT_{dgg})}; G_{dgt}(s) = \tfrac{K_{dgt}}{(1+sT_{dgt})}; \\ &G_{ae}(s) = \tfrac{K_{ae}}{(1+sT_{ae})}; \\ &G_{fc}(s) = \tfrac{K_{fc}}{(1+sT_{fc})}; G_b(s) = \tfrac{K_b}{(1+sT_b)} \end{aligned}\right\}. \tag{11}$$

where $K_{dgg}, K_{dgt}, K_{fc}, K_{ae}$, and $K_b, T_{dgg}, T_{dgt}, T_{ae}, T_{fc}$, and T_b are the gains and time constants of governor, turbine of diesel generator, fuel cell, aqua electrolyzer and battery, respectively. The values of all these parameters are given in the Appendix.

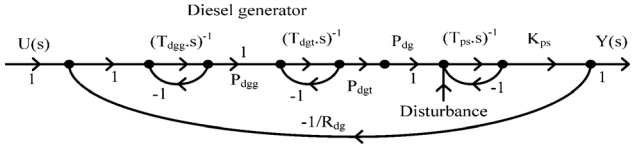

Fig. 4. Signal flow graph of the diesel generator.

C. Power and Frequency Deviation

The swing equation for a synchronous generator [24] is depicted in (12)

$$\Delta f = \frac{f_{sys}}{2Hs} \times [\Delta P_G - \Delta P_e]. \tag{12}$$

where

$$\begin{aligned} P_G &= P_W + P_s + P_{dg} + P_{fc} - P_{ae} \pm P_b \text{ and} \\ \Delta P_e &= \Delta P_L + D\Delta f. \end{aligned} \tag{13}$$

where f_{sys} = system frequency, Δf = deviation in frequency, P_G = Total power generation in the microgrid. P_W = Wind power generation, P_{S} = Solar power generation, P_{dg} = Diesel generator power output, P_{fc} = Fuel cell power output, P_{ae} = Aqua electrolyzer power output, P_b = Battery power output, P_L = Load disturbance, D = p.u load change with frequency, H = Inertia constant of the diesel generator.

Therefore, the transfer function for system frequency variation to per unit power deviation is given by (14).

$$\begin{aligned} G_{sys}(s) &= \frac{\Delta f}{(\Delta P_G - \Delta P_L)} = \frac{1}{\left[D + \left(\frac{2H}{f_{sys}}\right) s\right]} \\ &= \frac{K_{ps}}{(1 + sT_{ps})}. \end{aligned} \tag{14}$$

where K_{ps} (power system gain) and T_{ps} (power system time constant) are $1/D$ and $2H/(Df_{sys})$ respectively.

It is to be noted here that (12) is valid only when there is a synchronous machine in the microgrid. Therefore, the researchers should be careful in using (14) when they are simulating the microgrid.

D. Designing of P-f Droop for Different Controllable Sources in the Microgrid

In our paper [7] we have deliberated about the issue of designing the P-f droop for a microgrid. Since the model is same, the procedure adopted in this paper and [7] is identical. For quick understanding of the reader we are discussing the issue in brief. The P-f droop for different sources are related to each other as depicted in (15).

$$R_{dg} : R_{fc} : R_{ae} = \frac{1}{P_{fcrated}} : \frac{1}{P_{dgrated}} : \frac{1}{P_{aerated}}. \tag{15}$$

where R_{dg}, R_{fc}, R_{aq} are $P-f$ droop coefficient and $P_{dgrated}$, $P_{fcrated}, P_{aqrated}$ are the rated power of diesel generator, fuel cell and aqua electrolyzer respectively. Since the diesel generator has a second order transfer function, which may lead to instability; we started the design procedure from it. The closed loop signal flow graph of the diesel generator along with the power system is shown in Fig. 4.

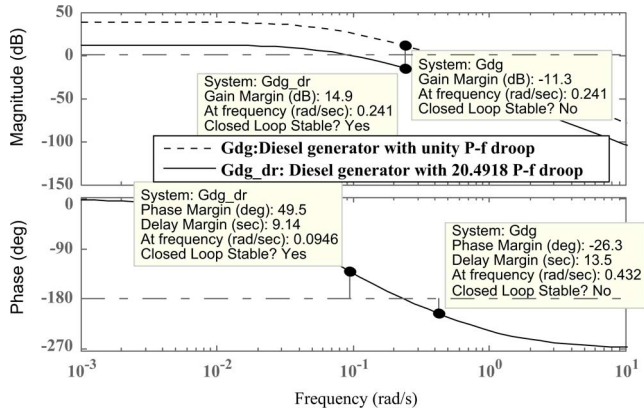

Fig. 5. Bode plot of the diesel generator.

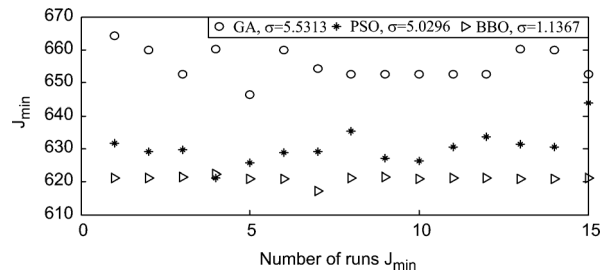

Fig. 6. The plot of $J_{\min}$ Vs number of runs for GA, PSO, and BBO.

The open loop transfer function of the diesel generator system, as written in (16), can be obtained from Fig. 4.

$$G_{dg} = \frac{K_{ps}}{(1 + sT_{dgt})(1 + sT_{dgg})(1 + sT_{ps})}. \tag{16}$$

Since there is a feedback path in Fig. 4 the characteristic equation for the closed loop system can be represented as in (17).

$$1 + G_{dg} \times \frac{1}{R_{dg}} = 1 + \frac{K_{ps}}{R_{dg}(1 + sT_{dgg})(1 + sT_{dgt})(1 + sT_{ps})}. \tag{17}$$

The bode plot of the transfer function corresponding to the diesel generator without P-f droop as depicted in (16) ($\mathrm{G_{dg}}$) and with P-f droop as shown in (17)($\mathrm{G_{dg_{dr}} = G_{dg}/R_{dg}}$) are presented in the Fig. 5. It can be concluded from the Fig. 5 that the diesel generator with "unity" droop destabilizes the power system by presenting negative phase and gain margins. However, for a droop of 20.4918 Hz/p.u. (power) the system is stable which can be ensured from the positive margins. Now, using (15) the P-f droop of fuel cell (200 kW) and aqua electrolyzer (100 kW) can be obtained. In our case they are 40.9836, 81.9672 respectively.

III. State Feedback LQR Control

LQR is a control scheme that gives the best possible performance with respect to a given performance criterion [10]. The performance criterion is a quadratic function of state vector and control input. In this method a feedback gain matrix "K" is designed to minimize the objective function "$\mathrm{J_{LQR}}$" in order to achieve a compromised solution between the control effort and the speed of response that will guarantee a stable system.

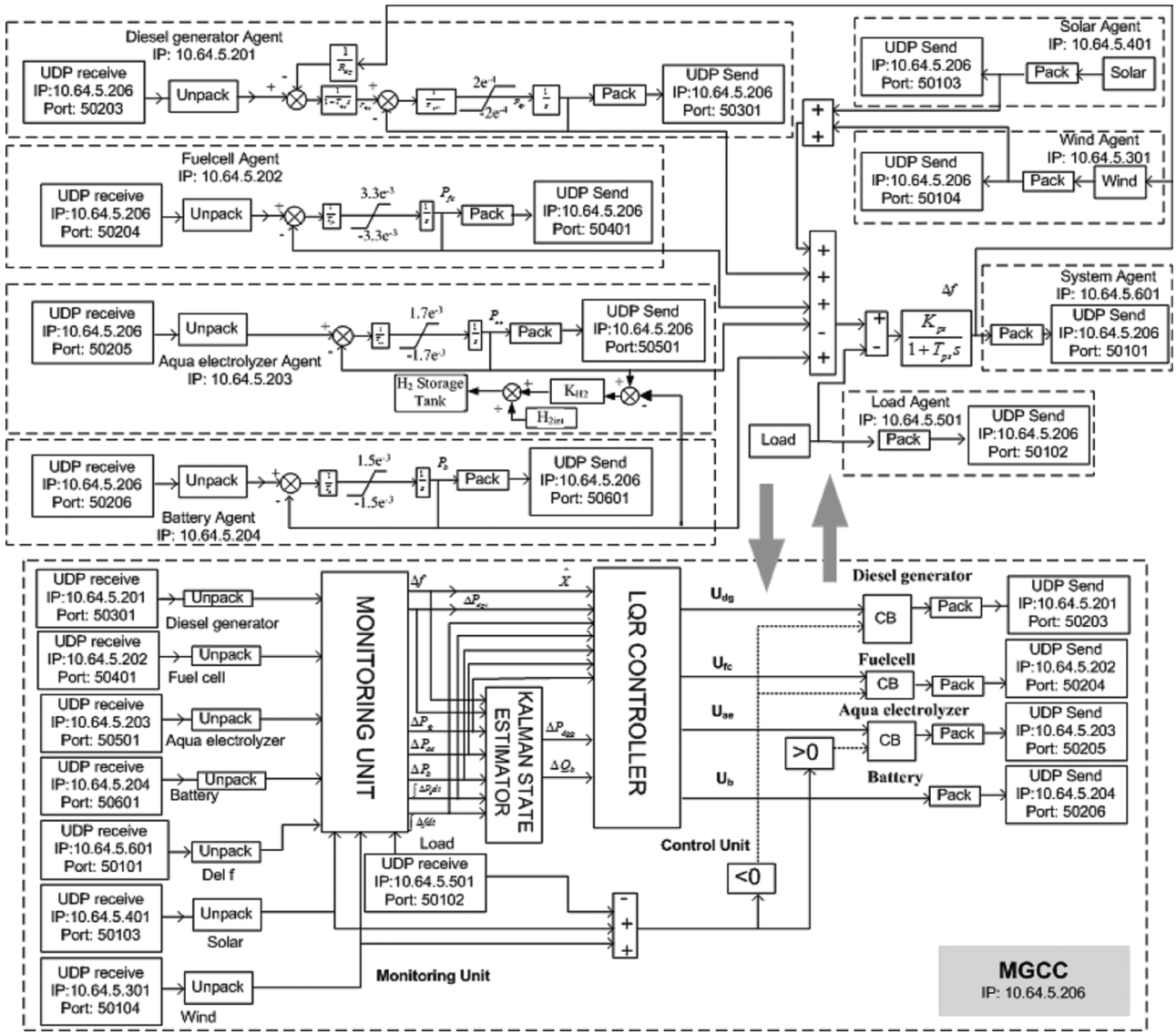

Fig. 7. The smart microgrid using MATLAB/SIMULINK.

For the given microgrid in Fig. 7 the state variable model can be described as below,

$$\dot{X} = AX + BU + \Gamma P_d \tag{18}$$

$$Y = CX. \tag{19}$$

where X, U, P_d and Y are the state, control, disturbance and output vectors respectively. The system matrices: A (state matrix), B (input matrix), Γ (disturbance matrix), and C (output matrix) are derived based on the microgrid parameters.

The state vector, also indicated in Fig. 7, for our case is as below,

$$X = \Big[\Delta f \Delta P_{dgg} \Delta P_{dgt} \Delta P_{fc} \Delta P_{ae} \Delta P_b \Delta Q_b \times \int \Delta P_b dt \int \Delta f dt\Big]^T. \tag{20}$$

Similarly, the control vector can be represented as below,

$$U = [\Delta U_{dg} \Delta U_{fc} \Delta U_{ae} \Delta U_b]^T. \tag{21}$$

In our case, the output Y is taken as Δf, $\int \Delta f dt$, ΔP_{dgt} (diesel generator turbine output), ΔP_{fc}, ΔP_{ae}, P_b and $\int P_b dt$ of the microgrid. Redefining the state variable set and control variable set as $\hat{X} = \dot{X}$, $\hat{U} = \dot{U}$ [10], we can remove the disturbance vector and hence can find the optimal control strategy such that the cost below is minimized.

$$J_{LQR} = \frac{1}{2}\int_0^\infty (\dot{X}^T Q \dot{X} + \dot{U}^T R \dot{U}). \tag{22}$$

The optimal control signals U that minimize the cost "$\mathrm{J_{LQR}}$" is as given in (23)

$$U = -KX. \tag{23}$$

where

$$K = R^{-1} B^T P. \tag{24}$$

with "P" being the solution of the algebraic matrix Riccati equation

$$A^T P + PA - PBR^{-1}B^T P + Q = 0. \tag{25}$$

Looking at (24) and (25) we can say that for each set of "Q" and "R" matrices there will be an unique "K" matrix which influences the control signal such that (22) is minimized. Therefore, the research challenge is in finding out the best set of "Q" and "R" that will regulate the desired variables (not necessarily the state variables) optimally. In this paper we want to minimize the frequency deviation by keeping the battery power at zero and state of the charge of the battery at its initial value in the steady state. Based on this philosophy a cost function has been formulated and depicted in (26).

$$J = \int t\left(|\Delta f|^2 + |\Delta P_b|^2 + |Q_b|^2\right)dt. \tag{26}$$

Hence, the need is now to obtain the set of "Q" and "R" that will minimize (26). Since, it is almost impossible to get the gradient of "J" with respect to "Q" and "R"; we have used some iterative techniques, to calculate "Q" and "R" so as to minimize "J."

The state feedback LQR formulation considered above suffers from the drawback that the optimal control law $U = -KX$ requires all states of the microgrid given in (20) to be measurable. A possible approach to overcome this difficulty is to estimate the unknown states based on the measured state variables Y , and use

$$U = -K\hat{X}. \tag{27}$$

where $\hat{X}$ denotes an estimate of the process state X. In this paper we have used Kalman estimator [10]. In our problem, out of the nine state variables depicted in (20) seven states such as Δf, $\int \Delta f dt$, ΔP_{dgt} (diesel generator turbine output), ΔP_{fc}, ΔP_{ac}, P_b and $\int P_b dt$ are considered as measureable, whereas, states ΔP_{dgg} (diesel generator governor output), ΔQ_b (battery state of the charge) are assumed to be unobservable.

IV. Tuning of Weightage Matrices "Q" and "R"

The calculation of optimal weightage matrices "Q" and "R" to be used in the Riccarti equation is the major research problem. It is generally obtained through trial-and-error method. This requires, testing of a large number of "Q" and "R" matrices to reach an acceptable solution. Even if we get a satisfactory response, still we are in dark whether there is some other "Q" and "R" which can perform better. Therefore, in this paper we have tried to formulate a systematic approach to design the "Q" and "R" matrices.

A. Bryson Method

Bryson [11] developed the simple iterative method based on the "inverse square" for the selection of the quadratic cost/weightage matrices "Q" and "R." The basic concept behind the technique is to normalize the contribution which the outputs and the control term may have within the quadratic cost function. This normalization is usually accomplished using the anticipated maximum values (or deviation) of the individual outputs and controls [11], [12] as discussed below.

$$Q = diag[q_1 q_2 q_3 \dots q_n]$$
$$R = diag[r_1 r_2 r_3 \dots r_m]$$

$$\text{Where } \left[q_i = \frac{1}{x_i^2(\max)}\right]_{i=1}^{n} \; and \; \left[r_j = \frac{1}{u_j^2(\max)}\right]_{j=1}^{m}. \tag{28}$$

Utilizing (28), with the help of (24) and (25) the optimal feedback gain "K" to minimize J_{LQR} given in (22) can be obtained. The "K" so obtained may not lead to a minimum "J" when calculated using (26). Hence, we need some iterative approach to reach at some optimal solution for "Q" and "R." As any iterative method requires some starting points as well as a disturbance, we have considered the "Q" and "R" obtained using Bryson's rule as the initial guess and a load increase of 5% as the disturbance.

B. Conventional Iterative Based Approach

In this paper, the "fminsearch" optimization procedure available in MATLAB [25] is used to carry-out the iterative based optimization to minimize "J" given in (26). The initial "Q" and "R" given to this algorithm are those obtained using (28) and depicted in the Appendix. It is found that using this algorithm it is possible to reach a minimum value of 686.3053 for the "J" given in (26). Besides, as this algorithm does not involve any random values, the solution is consistent across different runs. The optimized value of "Q" and "R" matrices corresponding to this method are given in the Appendix.

C. Evolutionary Algorithms Based Iterative Approach

Recently, many powerful evolutionary algorithm based iterative approaches have been developed for optimizing parameters in different engineering problems. From among them the optimization methods especially GA and PSO has been used widely. Recently the BBO has come to the research domain as an alternative evolutionary algorithm. Therefore, in this section we have tried to explore the capability of BBO as against GA and PSO in optimizing the "Q" and "R" matrices with initialization through the Bryson's method.

To compare the obtained optimal solution and its consistency for different algorithms the following experiment is carried out with repetitive run. To have a fair comparison between the considered algorithms we have restricted the number of cost function evaluations (J_{eval}) to 2500 and termed it as one run. This is considered as any evolutionary technique optimizes the variables based on the decisions obtained through J_{eval}. Fig. 6 depicts the variation of optimal "J" for different run whose starting points are the one indicated by the Bryson's rule.

From Fig. 6, it is observed that the standard deviation "σ" in the optimal results as well as the optimal solution is minimum in case of BBO as compare to GA and PSO. This indicates that BBO is a better algorithm which gives consistent results for different runs with better optimal solution. Besides, all the three evolutionary algorithms present better result as compared to the conventional algorithm. The details about the BBO algorithm are discussed in the following section.

V. Biogeography Based Optimization (BBO)

BBO [13] is a global optimization algorithm inspired by the distribution of species (biogeography). In BBO, each individual

is considered as a "habitat" with habitat suitability index (HSI), which is similar to the fitness of evolutionary algorithms, to measure the individual. An optimum solution is analogous to an island with a high HSI, and a poor solution indicates an island with a low HSI. The features of the high HSI solutions are shared by the low HSI solutions. Low HSI solutions accept a lot of new features from the high HIS solutions. In BBO, each individual has its own immigration rate I and emigration rate E. An optimal solution has higher immigration rate I and lower emigration rate E. The details about the BBO algorithm and its efficiency are discussed in [14], [15]. In this algorithm the parameters used for searching the total solution space is much higher. In case of BBO technique we assign each habitant with a set of variables to be optimized, i.e., elements of weightage matrices Q and R. Each species is allowed to take all possible values and the performance criterion presented in (26) is minimized.

The species for which the performance criterion is minimum in the last BBO iteration estimates the parameters to be used.

In this paper, the BBO algorithm is implemented with the following initialization.

i. In LQR control, the number of parameters $(p = 11)$ to be optimized. The 8 gains for state variables and 3 gains for control inputs.
ii. Number of habitants $(S = 50)$ to be used for searching the total region, Maximum Immigration rate $I = 1$, Maximum Emigration rate $E = 1$, Time step for probability rate conversion $\Delta t = 1$, Modification probability $P_{mod} = 1$, Mutation probability $P_{mut} = 0.005$, $\lambda_{lower} = 0$, $\lambda_{\text{upper}} = 1$, Number of elite $\text{variable} = 2$, Maximum number of $\text{iterations} = 50$.

VI. The Smart Microgrid

To achieve a simultaneous target of frequency control and proper energy management we have implemented the MAS philosophy into the microgrid [7], [26]. This method assigns an IP address to each entity (in our case all loads and sources) which is further called as an agent. The assigned IP address helps the server used as MGCC to establish a bidirectional information flow path between the agents and the MGCC in an analogues way as adopted in wide area control application discussed in [27]. This bidirectional data transfer is carried out using UDP/IP. The agents are associated with UDP send and UDP receive blocks to send and receive the data to and from the MGCC. The UDP send block consist of one input, the receiving agent's IP address and the address of the port through which the data is to be sent to the receiving agent. Similarly, the UDP receive block has one input, the sending agent's IP address and the address of the port through which the data is to be received by the receiving agent.

The monitored variables are sensed using suitable sensors and converted to a digital domain by analog to digital (A/D) converters and passed to the communication network. On the receiving end a digital to analog (D/A) converter will decode the instruction sent by the MGCC to the agents. The schematic of the smart microgrid, with all states and control variables being indicated, is shown in Fig. 7.

A. Microgrid Central Controller

The energy management function of the MGCC as envisaged in this paper is same as that of our paper [7]. Just for continuity of the text we are rewriting the rules governing the MGCC decision as proposed in [7].

R1) It is required to switch off the diesel generator and fuel cell and switch on the aqua electrolyzer when the aggregate power obtained from the renewable energy sources $(\text{wind} + \text{solar})$ is higher than the load. Similarly, the reverse would happen when the load is higher than the power produced from the renewable energy sources. This agrees to the concept of using renewable energy first.

R2) It is desirable to have an alarm when the pressure in the hydrogen tank is not sufficient to drive the fuel cell to produce power.

VII. Simulation Results and Analysis

Case 1: Sudden load increase by 5% when WECS is either in MPPT or participating in frequency control.

In this case the transient handling capacity of the WECS and battery, with different controllers tuned by BBO, for the frequency control of the microgrid is discussed. We have considered the scenarios when WECS is either in MPPT or participating in frequency control of the microgrid. The power response of WECS, battery and microgrid frequency deviation are shown in Fig. 8(a)–8(d). Looking at Fig. 8(a) and 8(b), we can ascertain that when the WECS is participating in frequency control the transient power is supplied by WECS instead of battery. This is due to the fact that WECS can release the kinetic energy almost instantaneously to support during the transient. However, due to limitation on discharging/charging current of a battery the power can not increase so quickly (modeled in the paper through GRC) for a battery energy storage system. Therefore, though the peak value of change in transient power, supplied from both the sources are almost same, the frequency deviation is quite large in the case when WECS is under MPPT. As a result, when WECS is used for frequency control we can have better frequency response as well as an extended life period for the battery.

Now comparing the frequency response for different controllers given in Fig. 8(d), we can establish that BBO-LQR is the best performing alternative. However, BBO-LQR with Kalman estimator also performs more or less same with BBO-LQR. The worst among the controllers is the *fminsearch*-LQR which shows a frequency deviation of 0.1 Hz. Further, from Fig. 8(a)–8(c) we can also observe that in steady state both the battery and wind are coming to their reference which implies that they are ready for the next transients in the system

Case2: Dynamic response of the smart microgrid for sudden increase in solar insolation by 3%.

The dynamic responses of the microgrid for a sudden increase in solar insolation by 3% are shown in Fig. 9(a)–9(b). The "Q" and "R" matrices are again tuned for this case with the same procedure adapted before.

Based on the master controller decision for this case, the diesel generator and fuel cell will not supply any power to the microgrid. The transients are handled by the WECS, the battery and the aqua electrolyzer. As a result, the total increase in

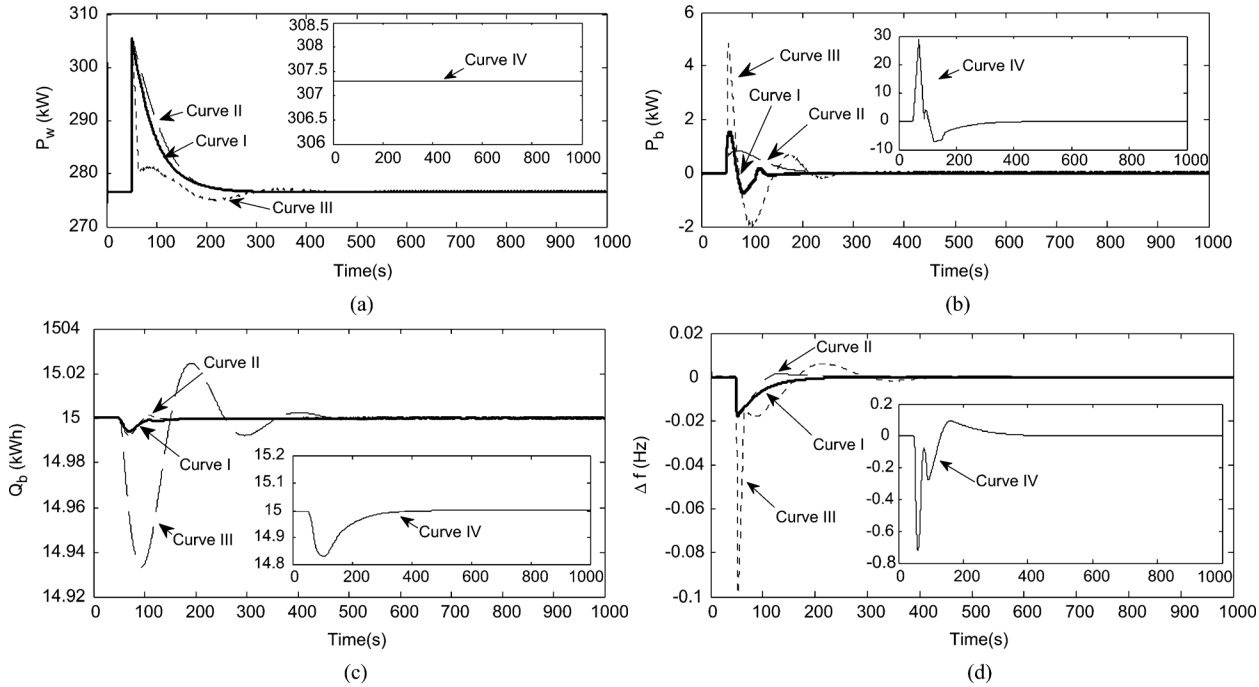

Fig. 8. (a) WECS power $\mathrm{P_w}$. (b) Battery power $\mathrm{P_b}$. (c) State of the charge of the battery $\mathrm{Q_b}$. (d) Frequency deviation Δf of the smart microgrid under 5% increase in load. Curve I—BBO-LQR with WECS participating in frequency control, Curve II—BBO-LQR + Kalman estimator with WECS participating in frequency control, Curve III—*fminsearch*-LQR with WECS participating in frequency control, Curve IV—*fminsearch* -LQR with WECS in MPPT.

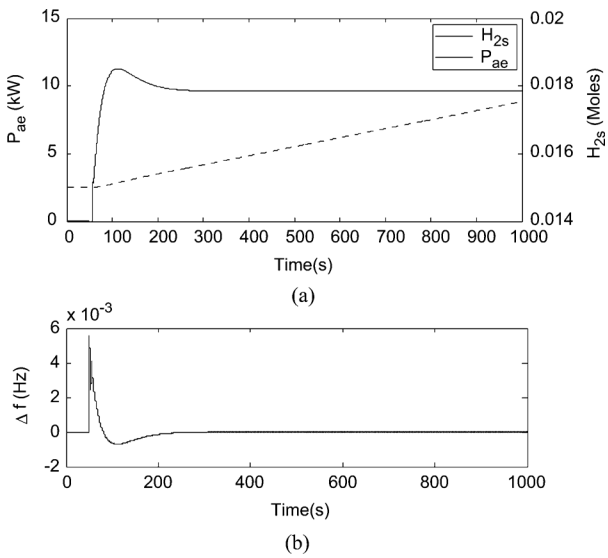

Fig. 9. (a) Aqua electrolyzer power P_{ae}, Hydrogen in storage tank $\mathrm{H_{2s}}$. (b) Frequency deviation Δf of the smart microgrid.

solar power is consumed by the aqua electrolyzer to produce hydrogen and sent for storage. This fact is clear by looking at Fig. 9(a). Further, from Fig. 9(b), it can be observed that the frequency deviation is very small and is within acceptable limit.

Case 3: Frequency response of the smart microgrid with data loss and wrong sequence of data in communication channel

Generally, the packet loss and the sequence missing condition may occur in UDP/IP. So, the effect of information loss or data sequence change has been studied in this case. For the 5% load increased situation, the MGCC will generate the control signal for the fuel cell. As shown in Fig. 10(a), this transmitted signal is lost at 205.2 s and there is a data exchange between 205.2 s with 205.4 s which is considered as wrong sequence. To address the data loss, as shown in Fig. 10, we have assumed that the previous data will continue to act as the reference. So the reference power to the fuel cell remains same during 205.1 s to 205.3 s which makes the effect of data loss over the frequency excursion almost negligible. In addition, as long as the time delay is small, problems in sequence will not affect the frequency excursion. Furthermore, the sequence will be taken care of by another layer, if the UDP/IP is adopted. As in this scheme there will be a time stamping, the receiver will receive the data only when it arrives at the receiver within a stipulated time frame, otherwise not. Frequency excursion presented in Fig. 10(b) confirms the above discussions showing that the frequency deviation is affected neither by data loss nor by wrong sequencing in received signal.

VIII. Conclusions

In this paper, BBO algorithm has been successfully implemented to tune the controller parameters such as "Q" and "R" matrices of the LQR controller. Kalman estimator has been implemented to tackle the issue of immeasurable states required by the LQR. It is observed that with WECS participating in frequency control the usage of battery reduces hence, increasing the life time and decreasing the capacity of the battery. For optimal usage of the microgrid resources the concept of smart microgrid is proposed based on MAS and UDP/IP. It is found that the data loss and wrong sequence associated with UDP/IP does not influence the performance of the controllable sources.

Appendix

Parameters for solar power

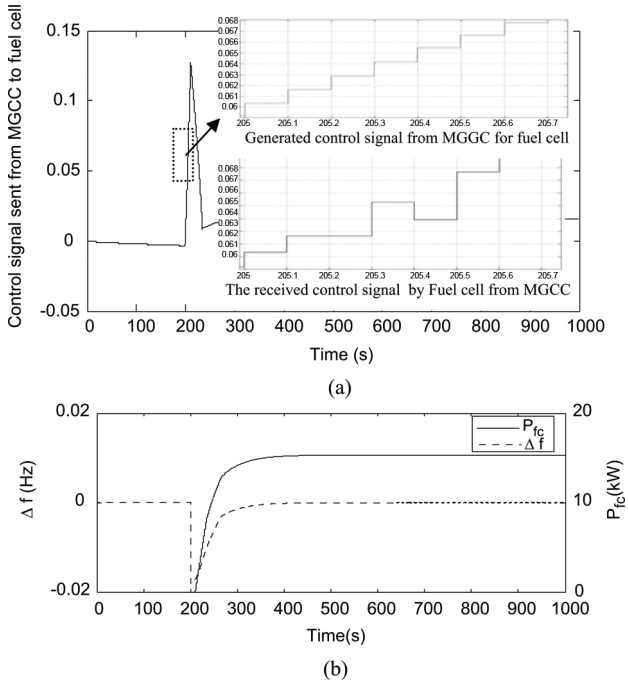

Fig. 10. (a) The control signals between MGCC and fuel cell. (The data loss and wrong sequence is shown in zoomed figure.) (b) Frequency deviation Δf of the microgrid, Fuel cell power $\mathrm{P_{fc}}$ under 5% increase in load.

$\mathrm{I_{rs}} = 1.2\mathrm{e}^{-7}$; $\mathrm{I_{scr}} = 8.03$; $\mathrm{T_r} = 300$; $\mathrm{T} = 320$; $\mathrm{K_t} = 0.0017$; $\mathrm{A} = 1.92$; $\mathrm{n_p} = 176$; $\mathrm{n_s} = 1500$; $\mathrm{K} = 1.3805\mathrm{e}^{-23}$; $\mathrm{q} = 1.610\mathrm{e}^{-19}$; $\mathrm{S} = 0.2$; $\mathrm{V_{dc0}} = 542.2651$ V; $\mathrm{K_s} = 1.7018$; $\mathrm{T_s} = 0.05$ s.

Nominal parameters of the microgrid

$\mathrm{f_{sys}} = 50$ Hz, Base Power $= 1$ MVA, $\mathrm{D} = 0.012$ MW/Hz, $\mathrm{H} = 5$ s; $\mathrm{T_{dgg}} = 2$ s, $\mathrm{T_{fc}} = 4$ s, $\mathrm{T_b} = 0.1$ s, $\mathrm{T_{ae}} = 0.2$ s, $\mathrm{T_{dgt}} = 20$ s, $\mathrm{K_{dgg}} = \mathrm{K_{dgt}} = \mathrm{K_{fc}} = \mathrm{K_b} = \mathrm{K_{ae}} = 1$, $\mathrm{GRC_{dg}} = 3\%$, $\mathrm{GRC_{ae}} = 10\%$, $\mathrm{GRC_{fc}} = 10\%$, $\mathrm{GRC_b} = 30\%$.

Optimal values of weightage matrices Q and R for 5% load increase disturbance

Bryson's initial values:

$\mathrm{R} = \mathrm{diag}(1./[30\ 30\ 30]\hat{}\,2)$;

$\mathrm{Q} = \mathrm{diag}(1./[0.001\ 30\ 30\ 30\ 30\ 15\ 0.001\ 0.001]\hat{}\,2)$;

fminsearch:

$\mathrm{R} = \mathrm{diag}([119.9967\ 1099.5489\ 2739.1767])$;

$\mathrm{Q} = \mathrm{diag}([999.9374\ 1096.9653\ 1140.65381\ 1118.9129\ 999.93431\ 0.12716\ 0.00614\ 0.29631])$;

Genetic Algorithms (GA):

$\mathrm{R} = \mathrm{diag}([97.1777\ 3819.5313\ 2299.8047])$;

$\mathrm{Q} = \mathrm{diag}([3177.7349\ 1091.9922\ 1098.6328\ 1181.44531\ 6189.4531\ 0.0609\ 0.0053\ 0.0852]$;

Particle Swarm Optimization (PSO):

$\mathrm{R} = \mathrm{diag}([99.1321\ 1147.0907\ 7355.9336])$;

$\mathrm{Q} = \mathrm{diag}([3792.9352\ 1122.5454\ 1070.2197\ 1170.3612\ 8886.1621\ 0.0125\ 0.0182\ 0.0421])$;

Biogeography Based Optimization (BBO):

$\mathrm{R} = \mathrm{diag}([90.94820\ 800.66927\ 1500.35488])$;

$\mathrm{Q} = \mathrm{diag}([4699.13011\ 1000.01100\ 1000.03500\ 1200.10006\ 7000.14373\ 0.01031\ 0.00101\ 0.10000])$;

Optimal values of weightage matrices Q and R for 3% increase in solar insolation

Bryson's intial values:

$\mathrm{R} = \mathrm{diag}(1./[18\ 18]\hat{}\,2)$;

$\mathrm{Q} = \mathrm{diag}(1./[0.001\ 18\ 18\ 15\ 0.001\ 0.001]\hat{}\,2)$;

fminsearch:

$\mathrm{R} = \mathrm{diag}([0.5033\ 0.9315])$;

$\mathrm{Q} = \mathrm{diag}([0.3872\ 35.9312\ 0.0214\ 1.7415\ 94.7832\ 0.0003])$;

Biogeography Based Optimization (BBO):

$\mathrm{R} = \mathrm{diag}([0.4388\ 4.9643])$;

$\mathrm{Q} = \mathrm{diag}([0.5379\ 45.0127\ 0.9849\ 9.0568\ 148.0881\ 0.0004])$;

REFERENCES

[1] S. P. Chowdhury, P. Crossley, S. Chowdhury, and E. Clarke, *Microgrids and Active Distribution Networks*. London, U.K.: IET, 2009.

[2] J. A. P. Lopes, C. L. Moreira, and A. G. Madureira, "Defining control strategies for microgrids islanded operation," *IEEE Trans. Power Syst.*, vol. 21, no. 2, pp. 916–924, May 2006.

[3] M. A. Hassan and M. A. Abido, "Optimal design of microgrids in autonomous and grid-connected modes using particle swarm optimization," *IEEE Trans. Power Electron.*, vol. 26, no. 3, pp. 755–769, Mar. 2011.

[4] I. J. Balaguer, Q. Lei, S. Yang, U. Supatti, and F. Z. Peng, "Control for grid-connected and intentional islanding operations of distributed power generation," *IEEE Trans. Ind. Electron.*, vol. 58, no. 1, pp. 147–157, Jan. 2011.

[5] R. Majumder, B. Chaudhuri, A. Ghosh, R. Majumder, G. Ledwich, and F. Zare, "Improvement of stability and load sharing in an autonomous microgrid using supplementary droop control loop," *IEEE Trans. Power Syst.*, vol. 25, no. 2, pp. 796–808, May 2010.

[6] L. Hari, M. L. Kotari, and J. Nanda, "Optimum selection of speed regulation parameters for automatic regulation control in discrete mode considering generation rate constraints," *IEE Proc. Gener., Transm., Distrib.*, vol. 138, no. 5, pp. 401–406, Sep. 1991.

[7] S. Mishra, G. Mallesham, and A. N. Jha, "Design of controller and communication for frequency regulation of a smart microgrid," *IET Renew. Power Gener.*, vol. 6, no. 4, pp. 248–258, Jul. 2012.

[8] I. Robandi, K. Nishimori, R. Nishimura, and N. Ishihara, "Optimal feedback control design using genetic algorithm in multimachine power system," *Electr. Power Energy Syst.*, vol. 23, no. 4, pp. 263–271, May 2001.

[9] O. Oral, L. Cetin, and E. Uyar, "A novel method on selection of Q and R matrices in the theory of optimal control," *Int. J. Syst. Control*, vol. 1, no. 2, pp. 84–9, Mar. 2010.

[10] H. W. Smith and E. J. Davison, "Design of industrial regulators: Integral feedback and feedforward control," *Proc. Inst. Elect. Eng.*, vol. 119, no. 8, pp. 1210–1216, Aug. 1972.

[11] A. E. Bryson and Y. Ho, *Applied Optimal Control*. New York: Hemisphere, 1975.

[12] M. A. Johnson and M. J. Grimble, "Recent trends in linear optimal quadratic multivariable control system design," *IEE Proc. Control Theory Appl.*, vol. 134, no. 1, pp. 53–71, 1987.

[13] D. Simon, "Biogeography-based optimization," *IEEE Trans. Evol. Comput.*, vol. 12, no. 6, pp. 702–713, Dec. 2008.

[14] A. Chattopadhyay and P. K. Bhattacharya, "Biogeography-based optimization for different economic load dispatch problems," *IEEE Trans. Power Syst.*, vol. 25, no. 2, pp. 1064–1077, May 2010.

[15] T. K. Das, G. K. Venayagamoorthy, and U. O. Aliyu, "Bio-inspired algorithms for the design of multiple optimal power system stabilizers: SPPSO and BFA," *IEEE Trans. Ind. Appl.*, vol. 44, no. 5, pp. 1445–1457, Sep./Oct. 2008.

[16] D. E. Godbereg, *Genetic Algorithm in Search, Optimization and Machine Learning Reading*. Reading, MA: Addison-Wesley, 1989.

[17] R. C. Eberhart and Y. Shi, "Particle swarm optimization: Developments, applications and resources," in *Proc. Congr. Evol. Comput.*, May 2001, vol. 1, pp. 81–86.

[18] Y. del Valle, G. K. Venayagamoorthy, S. Mohagheghi, J.-C. Hernandez, and R. G. Harley, "Particle swarm optimization: Basic concepts, variants and applications in power systems," *IEEE Trans. Evol. Comput.*, vol. 12, no. 2, pp. 171–195, Apr. 2008.

[19] P. Mitra and G. K. Venayagamoorthy, "An adaptive control strategy for DSTATCOM applications in an electric ship power system," *IEEE Trans. Power Electron.*, vol. 25, no. 1, pp. 95–104, Jan. 2010.

[20] W.-T. Lin, Y.-C. Yin, and L.-R. Chang-Chien, "Enhancing frequency response control by DFIGs in the high wind penetrated power systems," *IEEE Trans. Power Syst.*, vol. 26, no. 2, pp. 710–718, May 2011.
[21] N. R. Ullah, T. Thiringer, and D. Karlsson, "Temporary primary frequency control support by variable speed wind turbines potential and applications," *IEEE Trans. Power Syst.*, vol. 23, no. 2, pp. 601–612, May 2008.
[22] A. Yazdani and P. P. Dash, "A control methodology and characterization of dynamics for a photovoltaic (PV) system interfaced with a distribution network," *IEEE Trans. Power Del.*, vol. 24, no. 3, pp. 1538–1551, Jul. 2009.
[23] T. Senjyo, T. Nakaji, K. Uezato, and T. Funabashi, "A hybrid power system using alternative energy facilities in isolated island," *IEEE Trans. Energy Convers.*, vol. 20, no. 2, pp. 406–414, Jun. 2005.
[24] O. I. Elgerd, *Electric Energy System Theory: An Introduction*, 2nd ed. New York: McGraw-Hill, 1982.
[25] J. C. Lagarias, J. A. Reeds, M. H. Wright, and P. E. Wright, "Convergence properties of the nelder-mead simplex method in low dimensions," *SIAM J. Optim.*, vol. 9, no. 1, pp. 112–147, 1998.
[26] M. Pipattanasomporn, H. Feroze, and S. Rahman, "Multi-agent systems in a distributed smart grid: Design and implementation," in *Proc. IEEE/PES Power Syst. Conf. Expo.*, Mar. 2009, pp. 1–8.
[27] P. Mitra and G. K. Venayagamoorthy, "Wide area control for improving stability of a power system with plug-in electric vehicles," *IET Proc. Gener., Transm., Distrib.*, vol. 4, no. 10, pp. 1151–1163, 2010.

S. Mishra (M'97–SM'04) received the B.E. degree from University College of Engineering, Burla, Orissa, India, and the M.E. and Ph.D. degrees from Regional Engineering College, Rourkela, Orissa, India, in 1990, 1992, and 2000, respectively.

In 1992, he joined the Department of Electrical Engineering, University College of Engineering Burla, as a Lecturer, and subsequently became a Reader in 2001. Presently, he is a Professor with the Department of Electrical Engineering, Indian Institute of Technology Delhi, India. His interests are in soft computing applications to power system control, power quality, grid integration of renewable energy, microgrid, and smart grid.

Dr. Mishra has been honored with many prestigious awards such as the INAE Silver Jubilee Young Engineer Award in 2012, the INSA Young Scientist Medal in 2002, and recognition as the DST Young Scientist in 2001 to 2002, etc. He is a Fellow of Indian National Academy of Engineering, Institute of Engineering and Technology (IET), London, UK and Institute of Electronics and Communication Engineering (IETE), India.

G. Mallesham received the B.E degree in electrical engineering from the University College of Engineering, O.U, Hyderabad, A.P. and the M.Tech degree in control and instrumentation engineering from Indian Institute of Technology, Delhi.

He joined the Department of Electrical Engineering, University College of Engineering, O.U, Hyderabad, A.P., as an Assistant Professor in 2002. Currently he is a Ph.D scholar in Electrical Engineering Department, Indian Institute of Technology, Delhi. His research interests are system modeling, control and automation, soft computing, distribution generation, renewable energy, and smart microgrid.

P. C. Sekhar received the B.Tech degree from Jawaharlal Nehru Technological University Hyderabad, India, the M.Tech degree from National Institute of Technology Rourkela, India. Currently, he is a Ph.D research scholar at Indian Institute of Technology Delhi, New Delhi, India.

His research interests are soft computing applications to design and control of microgrid based power systems.